

# Radon and CO<sub>2</sub> as natural tracers to investigate the recharge dynamics of karst aquifers

Ludovic Savoy, Heinz Surbeck<sup>1</sup>, Daniel Hunkeler\*

Center for Hydrogeology and Geothermics (CHYN), University of Neuchâtel, Emile-Argand 11, CH-2009 Neuchâtel, Switzerland

## S U M M A R Y

This study investigated the use of radon (<sup>222</sup>Rn), a radioactive isotope with a half-life of 3.8 days, and CO<sub>2</sub> as natural tracers to evaluate the recharge dynamics of karst aquifer under varying hydrological conditions. Dissolved <sup>222</sup>Rn and carbon dioxide (CO<sub>2</sub>) were measured continuously in an underground stream of the Milandre test site, Switzerland. Estimated soil water <sup>222</sup>Rn activities were higher than baseflow <sup>222</sup>Rn activities, indicating elevated <sup>222</sup>Rn production in the soil zone compared to limestone, consistent with a <sup>226</sup>Ra enrichment in the soil zone compared to limestone. During small flood events, <sup>222</sup>Rn activities did not vary while an immediate increase of the CO<sub>2</sub> concentration was observed. During medium and large flood events, an immediate CO<sub>2</sub> increase and a delayed <sup>222</sup>Rn activity increase to up to 4.9 Bq/L and 11 Bq/L, respectively occurred. The detection of elevated <sup>222</sup>Rn activities during medium and large flood events indicate that soil water participates to the flood event. A soil origin of the <sup>222</sup>Rn is consistent with its delayed increase compared to discharge reflecting the travel time of <sup>222</sup>Rn from the soil to the saturated zone of the system via the epikarst. A three-component mixing model suggested that soil water may contribute 4–6% of the discharge during medium flood events and 25–43% during large flood events. For small flood events, the water must have resided at least 25 days below the soil zone to explain the background <sup>222</sup>Rn activities, taking into account the half-life of <sup>222</sup>Rn (3.8 days). In contrast to <sup>222</sup>Rn, the CO<sub>2</sub> increase occurred simultaneously with the discharge increase. This observation as well as the CO<sub>2</sub> increase during small flood events, suggests that the elevated CO<sub>2</sub> level is not due to the arrival of soil water as for <sup>222</sup>Rn. A possible explanation for the CO<sub>2</sub> trend is that baseflow water in the stream has lower CO<sub>2</sub> levels due to gas loss compared to water stored in low permeability zones. During flood event, the stored water is more rapidly mobilised than during baseflow with less time for gas loss. The study demonstrates that <sup>222</sup>Rn and CO<sub>2</sub> provides value information on the dynamics of groundwater recharge of karst aquifer, which can be of high interest when evaluating the vulnerability of such systems to contamination.

### Keywords:

Karst hydrogeology  
Soil  
Epikarst  
Radon  
Carbon dioxide  
Unsaturated zone

## 1. Introduction

Karst aquifers are an important water resource worldwide that is however considered to be highly vulnerable to contamination due to the presence of preferential flow paths along fissures and karst conduits. When evaluating the vulnerability of karst aquifers, it is important to understand the transit time of water and solutes from the land surface to the saturated zone and springs and to characterise groundwater flow paths. In groundwater studies, transit times and flow paths are frequently characterised using artificial tracers (Käss, 1998). While the method has the advantage that the input function is well defined, artificial tracers can generally only be applied over a small surface and the experiments are

time-consuming. Furthermore, it is difficult (memory effects) to repeat a tracer test at the same location to evaluate the reaction of a system under different hydraulic conditions. An alternative approach is the use of stable (<sup>18</sup>O, <sup>2</sup>H) and radioactive (<sup>3</sup>H) isotopes that are naturally presented in the rainwater and show a conservative behaviour. The response of environmental isotopes to precipitation events has been investigated at the catchment scale (Bakalowicz et al., 1974; Emblanch et al., 2003; Maloszewski et al., 1992, 2002; Rank et al., 1992) and at local scale within the unsaturated zone (Caballero et al., 1996; Chapman, 1992; Harmon, 1979; Perrin et al., 2003a; Yonge, 1985). These tracers were used to estimate mean transit times and to evaluate the respective contribution of different water sources (Katz et al., 1998; Lakey and Krothe, 1996; Lastennet and Mudry, 1987; Lee and Krothe, 2001; Maloszewski et al., 2002; Vervier, 1990). In several studies, it was observed that the isotopic response (<sup>18</sup>O, <sup>2</sup>H) at water arrival points in caves is highly buffered compared to rainfall, although

\* Corresponding author. Tel.: +41 32 718 2560.

E-mail address: daniel.hunkeler@unine.ch (D. Hunkeler).

<sup>1</sup> Present address: Nufilm, Fineta, CH-1792 Cordast, Switzerland.

discharge varies substantially (Caballero et al., 1996; Chapman, 1992; Perrin et al., 2003a). Similar results were obtained at the catchment scale for different karstic systems (Bakalowicz et al., 1974; Maloszewski et al., 2002). From these observations, sometimes combined with chemical parameters, it was concluded that during rainfall, freshly infiltrated water is stored in the karst aquifer and only a small part of it reaches the springs directly. While the method provides valuable information on the functioning of karst aquifers, the input signal can be complex complicating data interpretation. An alternative approach is the use of hydrochemical parameters to evaluate the dynamics of karst flow systems such as parameters related to limestone dissolution or more recently dissolved organic carbon (Hunkeler and Mudry, 2007). The results from natural tracer studies are often evaluated using a two component mixing model (Lahey and Krothe, 1996; Mahler and Garner, 2009; Pronk et al., 2009) to quantify the contribution of water that was stored in the system (pre-event water) and of freshly infiltrated rain water (event water) to discharge. In several studies, it was observed that high-flow events consist of a large amount of pre-event water (Lahey and Krothe, 1996; Pronk et al., 2009). Storage may take place in the deep phreatic zone or in the soil and epikarst zone (Williams, 2008). So far only a few studies have attempted to identify the storage location (Lee and Krothe, 2001). These studies have mainly relied on the measurement of limestone related parameters including the  $\delta^{13}\text{C}$  of dissolved inorganic carbon, which can however not yet be measured continuously.

This study focuses on the use of dissolved  $^{222}\text{Rn}$  and  $\text{CO}_2$  as natural tracers to evaluate the dynamics of transfer of water from soil to the saturated zone of karst aquifers.  $^{222}\text{Rn}$  is an attractive tracer for karst hydrogeology because its half life (3.8 days) corresponds to the time scale of rapid flow components in karst systems and due its inert behaviour as a noble gas (Criss et al., 2007).  $^{222}\text{Rn}$  is produced by  $\alpha$ -decay of  $^{226}\text{Ra}$ . At several locations, such as the western Jura mountains (Surbeck, 1992) or in Mediterranean regions (Laubenstein and Magaldi, 2008; Tadolini and Spizzico, 1998), elevated activities of  $^{226}\text{Ra}$  and other radioisotopes have been observed in soils compared to the underlying limestone. In the western Swiss Jura, where the study area is located,  $^{226}\text{Ra}$  activities around 5–35 Bq/kg were measured in Malm limestone while soils contained 300–1000 Bq/kg of  $^{226}\text{Ra}$ . This enrichment is likely due to the release of radionuclides during limestone weathering followed by their accumulation in clay minerals, iron-oxides and organic matter of the soil (Laubenstein and Magaldi, 2008; Von Gunten et al., 1996). Due to the high  $^{226}\text{Ra}$  activity and because  $^{226}\text{Ra}$  is located at the surface of grains, elevated  $^{222}\text{Rn}$  activities are expected in soil water compared to water that has been stored in limestone (Fig. 1). Indeed, in laboratory batch experiments, higher  $^{222}\text{Rn}$  activities were detected in water samples in contact with Terra Rossa soil samples compared to water samples in contact with limestone (Tadolini and Spizzico, 1998). Furthermore, similar concentration patterns of  $\text{CO}_2$  and  $^{222}\text{Rn}$  in the shallow unsaturated zone of a karst aquifer also suggested that  $^{222}\text{Rn}$  originated from the soil zone similarly as  $\text{CO}_2$  (Batiot-Guilhe et al., 2007).  $^{222}\text{Rn}$  has relatively high solubility in water with a Henry coefficient (ratio of the  $^{222}\text{Rn}$  activity (Bq/l) in water versus gas phase) of about 0.35 at 10 °C (Clever, 1979). Therefore,  $^{222}\text{Rn}$  produced in the soil zone will be partly present in aqueous phase and it is expected that  $^{222}\text{Rn}$  will be flushed into karst systems during rainfall events.  $^{222}\text{Rn}$  has been used as a tracer to investigate the air movement in karst systems based on continuous gas phase measurement (Batiot-Guilhe et al., 2007; Fernandez-Cortes et al., 2009). In a study of the Areuse spring, Switzerland, Eisenlohr and Surbeck (1995) observed that the  $^{222}\text{Rn}$  activity increases after the discharge increase suggesting a higher  $^{222}\text{Rn}$  production in the infiltration zone compared to the aquifer itself. In a different study (Falcone et al., 2008),  $^{222}\text{Rn}$  was used to quantify the

residence time of groundwater in unsaturated limestone where little  $^{222}\text{Rn}$  production occurs based on its exponential decay using discrete water samples.

$\text{CO}_2$  is mainly produced by the soil biological activity. The dissolved  $\text{CO}_2$  concentration of water infiltrating into karst systems can decrease by dissolution of carbonate minerals or due to degassing of  $\text{CO}_2$  (Fig. 1). Several studies have discussed the origin and behaviour of  $\text{CO}_2$  in the atmosphere of karstic systems (Baldini et al., 2006; Batiot-Guilhe et al., 2007; Bourges et al., 2001; Fernandez-Cortes et al., 2009). In these studies  $\text{CO}_2$  concentration typically varied between 2% and 5 vol.%  $\text{CO}_2$ . Other studies focussed on dissolved  $\text{CO}_2$  concentrations in karst (Liu et al., 2004; Vesper and White, 2004) and epikarst (Liu et al., 2007) springs. In case of concentrated infiltration via sinkholes,  $\text{CO}_2$  concentrations can decrease during heavy rainfall due to a dilution effect (Liu et al., 2004, 2007). However, during low intensity rainfall and dispersed infiltration, the effect of flushing  $\text{CO}_2$ -rich soils can dominate over dilution and the  $\text{CO}_2$  level increases in springs (Liu et al., 2007; Vesper and White, 2004) or in diffuse flow fractured media (Liu et al., 2004). For example in a karst springs in Kentucky/Tennessee (Vesper and White, 2004), dissolved  $\text{CO}_2$  concentrations increased after the maximum discharge was reached during storm flow, which was explained by diffuse infiltration through  $\text{CO}_2$ -rich soils lagging behind quickflow from a sinkhole. Hence, similarly as  $^{222}\text{Rn}$ ,  $\text{CO}_2$  can serve as a natural tracer to evaluate flowpaths in karst systems.

This study was carried out at the Milandre karst system in the Swiss Jura. The Milandre karst system is characterised by diffuse infiltration, a 40–80 m thick unsaturated zone and a well developed epikarst (Kovacs and Jeannin, 2003). The study goes beyond previous studies in karst systems in several ways.  $^{222}\text{Rn}$  and  $\text{CO}_2$  were measured continuously in the aqueous phase over nearly two years in contrast to previous studies that only included discrete sampling or only focussed on individual flood events. This approach made it possible to study a number of flood events of variable intensity. Rather than measuring at the spring where the hydrochemical response can be strongly affected by mixing of water from different subcatchments (Perrin et al., 2007), the measurements were carried out directly in an underground stream draining a smaller subsection of the karst system. In addition to  $^{222}\text{Rn}$  and  $\text{CO}_2$ , the discharge of the underground river, electrical conductivity and temperature of water were recorded. Furthermore, some measurements of the  $^{222}\text{Rn}$  activity and  $\text{CO}_2$  concentrations in gas samples from the soil and epikarst zone were carried out. Based on the measured  $^{222}\text{Rn}$  activities and electrical conductivity, the contribution of pre-event and event water to discharge during flood events of variable intensity was quantified. The pre-event water was separated into water stored in the soil zone and water stored in the limestone aquifer.

## 2. Study area

The Milandre test site is situated in the Swiss Jura, 8 km N–W of Porrentruy (Kovacs and Jeannin, 2003; Perrin et al., 2003b). The catchment area, estimated to be on the order of 13 km<sup>2</sup>, is drained by the Milandre karst network (Fig. 2). The springs of the system consist of the Saivu spring, with a discharge between 20 and 200 L/s, the Bame temporary spring with a discharge reaching 1500 L/s and the La Font intra-alluvial spring. The catchment is divided in four sub-systems corresponding to the three most important underground tributaries (Milandrine upstream, Droite tributary and Bure tributary) and the la Font watershed (unknown part of the cave system). The Milandre karst network is developed in the Rauracian limestone overlying the impermeable Oxfordian marls. The area receives around 1000 mm annual

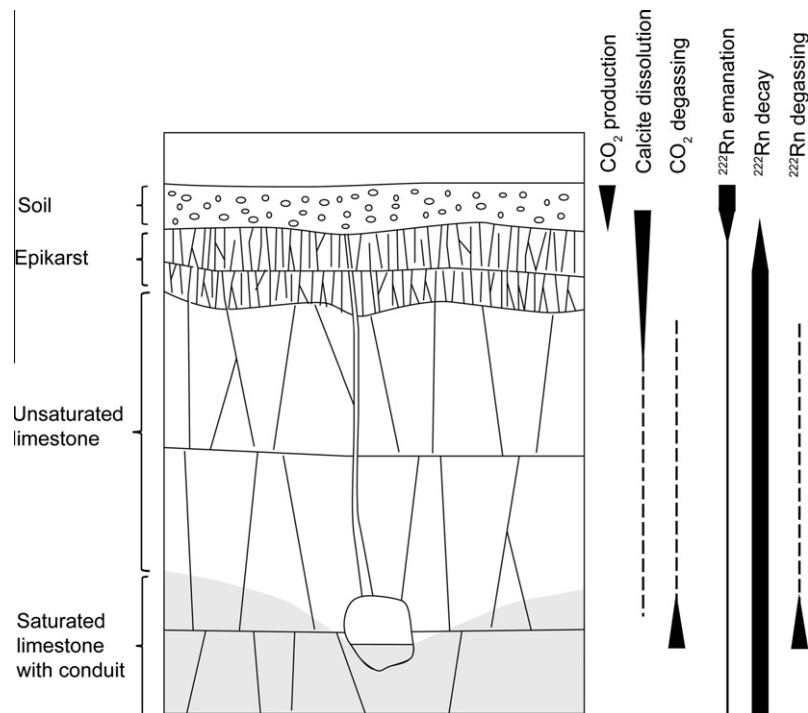


Fig. 1. Processes influencing <sup>222</sup>Rn activity and dissolved CO<sub>2</sub> concentration in karst system.

precipitation that recharges the aquifer mainly by diffuse infiltration (Kovacs and Jeannin, 2003; Perrin et al., 2003a). The unsaturated zone is about 40–80 m thick. The saturated zone is thin near the principal drains (a few metres) but can reach 30–40 m in low permeability zones. Access to the cave is possible by a series of two 20 m deep shafts. The entrance of the cave is closed by a door avoiding air circulation. The soil thickness varied between 1.1 and 3.4 m in boreholes drilled in the study zone (Fig. 2). This study focuses on the Milandre upstream tributary (20–600 L/s) which drains a catchment area of about 4.6 km<sup>2</sup> (30% cultivated land, 30% forests, 40% meadows) and corresponds to the most upgradient part of the system that is still accessible. The sampling location is about 55 m below the surface and corresponds to the interface between the saturated and unsaturated zone. A previous study has shown that the Milandre underground stream is saturated with respect to calcite even during high-flow events of up to 400 L/min (Perrin, 2003). Events above 400 L/min did not occur during this study.

### 3. Sampling and data acquisition

Soil gas samplers were installed to investigate the <sup>222</sup>Rn and CO<sub>2</sub> distribution in the infiltration zone of the Milandre site. Seven soil boreholes and one epikarst borehole were drilled in fields with different land use (pasture or forest) upgradient of the sampling and continuous monitoring site (Fig. 2). The depth of the boreholes depends of the soil thickness and the epikarst alteration and varies between 1.6 m and 3.7 m. The borehole diameter was 10 cm and they were filled with successive 30 cm layers of gravel and bentonite. Each gravel layer is connected to the surface with an aluminium tube ( $\varnothing = 6$  mm) and closed with rubber stoppers. The epikarst borehole is located in forest with less than 30 cm soil and reaches a depth of 15 m. It has two separate screened intervals, 0–5 m (Epikarst shallow) and 5–15 m (Epikarst deep). Each part of the borehole is connected to the surface with an aluminium tube ( $\varnothing = 6$  mm). Between September 2001 and August 2002, nine soil

CO<sub>2</sub> measurement campaigns were carried out at intervals between 1 and 2 months. Due to limited instrument availability and because the measurement is very time-consuming, <sup>222</sup>Rn activity measurements in the soil were only done once in August 2002.

Gas samples were taken using a peristaltic pump after purging several times the internal volume of the aluminium tubes. Gaseous CO<sub>2</sub> concentrations were determined by IR absorption using an Anagas CD 98 HR instrument (Environmental Instrument, England) with an integrated pump. Gas was pumped until a stable CO<sub>2</sub> concentration was observed for more than one minute. Gaseous <sup>222</sup>Rn was determined using a portable Lucas-cell based instrument (RDA-200, Scintrex, Canada). 600 ml of gas was pumped to purge and fill the Lucas cell (180 ml). After 5 min delay to allow for production of <sup>222</sup>Rn daughters and decay of external luminescence, the <sup>222</sup>Rn was measured during 10 min.

The most upstream part of the Milandrine underground stream (Fig. 2) was equipped with a continuous recording station for <sup>222</sup>Rn activity and CO<sub>2</sub> concentrations in parallel with discharge, specific conductivity and water temperature measurement. Data were acquired between September 2002 and May 2005 with a measurement interruption for <sup>222</sup>Rn and CO<sub>2</sub> between November 2002 and June 2003. The measurements in the soil zone and in the underground river were not carried out during the same year since the same measurement cell was used for gas and aqueous phase measurement. Continuous water level and conductivity measurements were carried out with pressure and conductivity probes. The discharge was calculated from the water level using the water level-discharge relationship obtained from occasional gauging experiments. For continuous measurement of dissolved <sup>222</sup>Rn, a closed circuit of air-filled semipermeable polypropylene tubing was immersed directly into the water of the river (Surbeck, 1996). Every 30 min (time necessary for equilibrium with dissolved gases in water) the gas in the tube was pumped (200 ml/min) through the detector. A Lucas-cell coupled to a photomultiplier detector was used to measure the <sup>222</sup>Rn concentration

in the air circuit. A concentration of 1 Bq/l in the water typically leads to 50 counts/min. For an integration time of 30 min, the standard deviation is 3% at 1 Bq/l and the detection limit is at 0.1 Bq/l. CO<sub>2</sub> is determined in the same closed air circuit by IR absorption, in series with the <sup>222</sup>Rn detector. The standard deviation is 0.05 vol.% at 1 vol.%.

The <sup>222</sup>Rn detector and the CO<sub>2</sub> sensor were packed together with the pump and electronics in a small watertight box. Thanks to the power dissipated and a styrofoam insulation, the temperature in the box stayed slightly above the outside temperature (10 °C+/-0.3 °C). As long as the outside temperature does not fall considerably below the water temperature there is no risk of condensation inside the box. In a cave where air temperature and water temperature are very similar, there is thus no need for a desiccant in the closed air loop. To calibrate the continuous measurement system, batch samples were taken in the river during different discharge conditions to cover the variations of <sup>222</sup>Rn and CO<sub>2</sub> levels. Batch samples were taken in 20 ml glass vials (PTFE/silicone septum cap). In the laboratory, <sup>222</sup>Rn was extracted with an organic solvent/scintillator cocktail (Maxilight, Hidex Oy, Finland) and after 3 h, <sup>222</sup>Rn and <sup>222</sup>Rn decay products were determined by liquid scintillation counting (LSC). The LSC-instrument (Triathler, Hidex Oy, Finland) ensures an efficient alpha/beta separation, leading to a low background count and thus to a low detection limit of 0.2 Bq/l for a measuring time of 1000 s. CO<sub>2</sub> in batch samples was determined by bubbling air through a 20 ml sample and measuring the CO<sub>2</sub> concentration in a closed air circuit by IR absorption (Texas Instruments Sensor, USA).

#### 4. Calculations

A three-component hydrograph separation was carried out. In a first step, pre-event and event water was separated based on the electrical conductivity using the following mixing equation:

$$f_E = \frac{C - C_{PE}}{C_E - C_{PE}} \quad (1)$$

where  $f_E$  is the fraction of freshly infiltrated event water,  $C$  the electrical conductivity measured at the sampling point,  $C_{PE}$  the electrical conductivity of pre-event water set equal to baseflow values and  $C_E$  the electrical conductivity of rainwater. The latter was set to 50 µS/cm assuming that only minor calcite dissolution occurs during rapid infiltration.

In a second step, the pre-event water was further subdivided into water stored in the soil zone and water stored in limestone based on the <sup>222</sup>Rn activity. The calculation made use of the following equation:

$$f_S = \frac{(C - C_L) - f_E \cdot (C_E - C_L)}{C_S - C_L} \quad (2)$$

where  $f_S$  is the fraction of water stored in the soil zone,  $C$  is the <sup>222</sup>Rn activity at the sampling point,  $C_E$  the <sup>222</sup>Rn activity in freshly infiltrated rain water,  $C_L$  the <sup>222</sup>Rn activity of water that has resided in limestone and  $C_S$  the <sup>222</sup>Rn activity of water stored in the soil zone.  $C_L$  was set to the baseflow <sup>222</sup>Rn activity and  $C_S$  to the <sup>222</sup>Rn activity calculated based on the average <sup>222</sup>Rn activity in soil using Henry's law and a dimensionless Henry coefficient of 0.35 at 10 °C (Clever, 1979). Since it is not known to what extent freshly infiltrated rain water dissolves <sup>222</sup>Rn during its passage through soil, the calculation was carried out for a range of <sup>222</sup>Rn activities corresponding to 0.25–0.75% of the equilibrium activity with respect to the gas phase. Based on the calculate fractions and discharge value for each measurement event, the total water volume for each of the three sources of water was calculated and transformed into mm water column by dividing it by the catchment area.

## 5. Results

### 5.1. Radon and CO<sub>2</sub> in soils

In the seven soil boreholes and the epikarst borehole, <sup>222</sup>Rn activities varied between 0.3 (+/-0.02) Bq/l and 68.6 (+/-0.3) Bq/l (Fig. 3). The <sup>222</sup>Rn activities decreased towards the land surface due to gas loss to the atmosphere by diffusion. In the sampling points located below the soil zone, <sup>222</sup>Rn activities were still elevated because some <sup>222</sup>Ra rich weathering products might have accumulated in the most superficial part of the epikarst or due to downward diffusion of <sup>222</sup>Rn. In the epikarst boreholes, smaller <sup>222</sup>Rn activities than in the soil were measured with 5.5 Bq/l for Epikarst shallow and 1.2 Bq/l for Epikarst deep, respectively. These data illustrate that elevated <sup>222</sup>Rn activities only occur in the top part of the epikarst while in deeper zones <sup>222</sup>Rn production is low. Hence, elevated <sup>222</sup>Rn activities are mainly characteristic of water stored in the soil zone.

Monthly CO<sub>2</sub> sampling campaigns were carried out in the same boreholes as for <sup>222</sup>Rn measurement. In all soil boreholes (Fig. 3), the CO<sub>2</sub> concentration generally increased with depth. The CO<sub>2</sub> concentrations showed strong annual variations with the highest levels at the end of the summer and the lowest at the end of the winter (data not shown). The annual mean CO<sub>2</sub> concentration varied between 1.73 and 3.49 vol.% for the different sites with no apparent link to land use (Table 1). Minimal values (end of winter) varied between 0.31 and 1.1 vol.% while maximal values (end of summer) were between 2.73 and 5.10 vol.% (Table 1). The amplitude of CO<sub>2</sub> concentrations ranged from 1.70 to 4.44 vol.% For the Epikarst deep borehole, the annual mean CO<sub>2</sub> concentration was 2.66 vol.% and corresponded to the average annual value for soil boreholes but with a lower amplitude (2.02 vol.%, Table 1). The minimal value observed in Epikarst deep during the end of winter is 1.58 vol.% and the maximal value (end of summer) 3.60 vol.%. The seasonal variation of the CO<sub>2</sub> concentration is linked to temperature variations with lower temperatures in winter leading to lower CO<sub>2</sub> concentrations due to lower microorganisms activity, less roots respiration and less decay of natural organic matter as already demonstrated in previous studies (e.g. Reardon et al., 1979). The smaller amplitude of the CO<sub>2</sub> concentration in deep epikarst suggests that the seasonal variations were buffered with depth.

### 5.2. <sup>222</sup>Rn and CO<sub>2</sub> during base flow and flood events in the underground stream

The results from continuous monitoring of the Milandrine underground stream are presented in three different groups depending on stream discharge: (1) base flow and small flood events with discharge less than 200 L/s; (2) medium flood events with discharge comprised between 200 L/s and 400 L/s; (3) large flood events with discharge above 400 L/s. A flood event is defined as a period during which the discharge is above the baseflow value.

#### 5.2.1. Base flow

During summer 2003 (between July 1st and August 28th), a long period of low rainfall occurred (105 mm in 65 days). In the Milandrine stream, the flow was very low (mean 16.7 L/s) and some small flood events with a maximum discharge less than 60 L/s were recorded (Fig. 4a). A mean <sup>222</sup>Rn activity of 3.2 Bq/l (min 2.9 Bq/l and max 4 Bq/l) and a mean CO<sub>2</sub> concentration of 2.2 vol.% (min 1.9 vol.% and max 2.6 vol.%) were measured (Fig. 4a). During summer 2004 (Fig. 4b), there was also a period of low rainfall (55.9 mm in 30 days) with a mean <sup>222</sup>Rn activity of 4 Bq/l (min 3.2 Bq/l, max 4.6 Bq/l) and mean CO<sub>2</sub> concentration

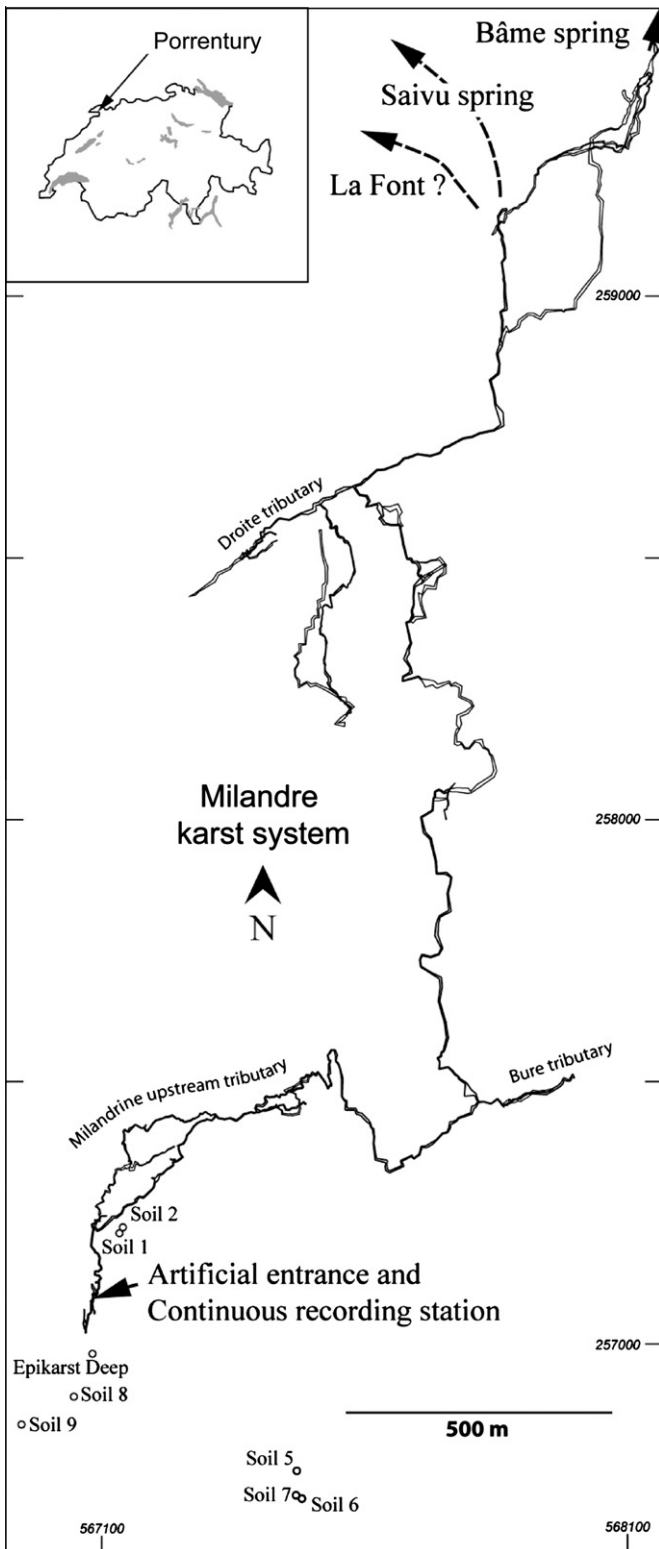


**Fig. 2.** Location of Milandre karst system with map of the Milandre cave. Location of boreholes and of continuous recording station (discharge, electric conductivity,  $^{222}\text{Rn}$  and  $\text{CO}_2$ ).

of 2.5 vol.% (min 2.2 vol.%, max 2.8 vol.%). During both periods, the electrical conductivity was constant at about  $630 \mu\text{s}/\text{cm}$ .

The  $\text{CO}_2$  level of water stored in limestone can be estimated based on the  $\text{CO}_2$  levels at the end of baseflow periods ( $<40 \text{ L/s}$ ). The average  $\text{CO}_2$  concentration and amplitude was even lower than in the deep epikarst borehole (Table 1). Thus the amplitude of  $\text{CO}_2$

variations seems to decrease from soil to epikarst to river, which can be explained by mixing of water in the epikarst and saturated zone of the aquifer leading to a  $\text{CO}_2$  concentration in the river during baseflow close to the annual average. In addition, dissolution of carbonates and degassing of  $\text{CO}_2$  in the conduits likely also contribute to smoothing of the  $\text{CO}_2$  concentration and lower levels of  $\text{CO}_2$  in deeper zones.

#### 5.2.2. Small flood events

On July 27th 2003, a flood event was observed after 15.9 mm rainfall (Fig. 5a). The maximum discharge (55 L/s) of the Milandre Stream was observed about 8 h after the maximum rain intensity. The  $^{222}\text{Rn}$  activity showed no changes (constant level at 3.2 Bq/l) but the  $\text{CO}_2$  concentration increased by 0.5 vol.% from 2.16 vol.% to 2.63 vol.% (Fig. 5a). The electrical conductivity was about  $630 \mu\text{s}/\text{cm}$  with no variations (Fig. 5a).

On October 9th 2004, a flood occurred after 25 mm rainfall (Fig. 5b). The discharge of the Milandre river increased about 4 h after the start of the rainfall. The discharge reached 95 L/s, the  $^{222}\text{Rn}$  level was stable (mean  $3.8 \pm 0.2 \text{ Bq/l}$ ) and  $\text{CO}_2$  concentration increased by 0.7 vol.% from 2.7 vol.% to 3.4 vol.% (Fig. 5b). The electrical conductivity was about  $630 \mu\text{s}/\text{cm}$  without significant variation.

#### 5.2.3. Medium flood events

On September 11th 2002, a flood event started after 21.2 mm rainfall during 3 h and a second discharge peak was observed after 11.8 mm rain during 12 h (Fig. 6a). Two days before the flood, 8.1 mm rainfall was measured but no flood was observed. The maximum discharge for the first peak (229 L/s) was observed about 9 h after the maximum rain intensity. In contrast to the small flood events, the  $^{222}\text{Rn}$  activity showed a significant increase of 0.9 Bq/l and the  $\text{CO}_2$  concentration an increase by 0.9 vol.% from 2.5 vol.% to 3.4 vol.% (Fig. 6a). The  $\text{CO}_2$  increase coincided with the discharge increase. The  $^{222}\text{Rn}$  increase is observed 8 h after the beginning of the flood and the  $^{222}\text{Rn}$  maximum 13 h after the maximum flow of the second peak, during decreasing discharge.

On June 1st an increased in discharge by 100 L/s was observed after 26.3 mm rainfall throughout the day. 10 h later stronger rainfall (44.1 mm) lead to an increase of the discharge to a maximum value of 341 L/s. Discharge increased about 7 h after the start of the first rainfall and 6 h after the second rainfall event. During the first discharge increase a small  $\text{CO}_2$  increase (2.4–2.7 vol.%) was observed. 9 h after the beginning of the second flood, a  $^{222}\text{Rn}$  increase was observed. The maximum  $^{222}\text{Rn}$  activity (4.94 Bq/l) was observed 16 h after the maximum discharge of the second peak. The  $\text{CO}_2$  increase coincided with the initial discharge increase. The electrical conductivity is about  $630 \mu\text{s}/\text{cm}$  and increases with the discharge. The increase in the  $\text{CO}_2$  concentration was smaller in the June flood event than in the September event, which is likely due to higher  $\text{CO}_2$  levels in soil and epikarst in September.

#### 5.2.4. Large flood events

The October 16th 2002 flood event corresponded to a rainfall of 102.6 mm during 7 days (Fig. 7a). This event can be separated in four successive flood event of increasing magnitude. The first discharge peak started after 14.4 mm rainfall during 24 h and reaches 172 L/s. A small  $\text{CO}_2$  increase by 0.6 vol.% from 3.3 to 3.9 vol.% was observed while no  $^{222}\text{Rn}$  increase occurred similarly to the small flood events described above. After 24 h without rainfall, a series of three larger discharge peaks followed (max 515 L/s, 478 L/s and 579 L/s, respectively). Each of the three flood peaks was accompanied by an increase in the  $^{222}\text{Rn}$  activity, which occurred with a delay of 4–8 h. The  $\text{CO}_2$  increased by 0.2 vol.% (3.6–3.8 vol.%) immediately after beginning of the first large flood peak and then

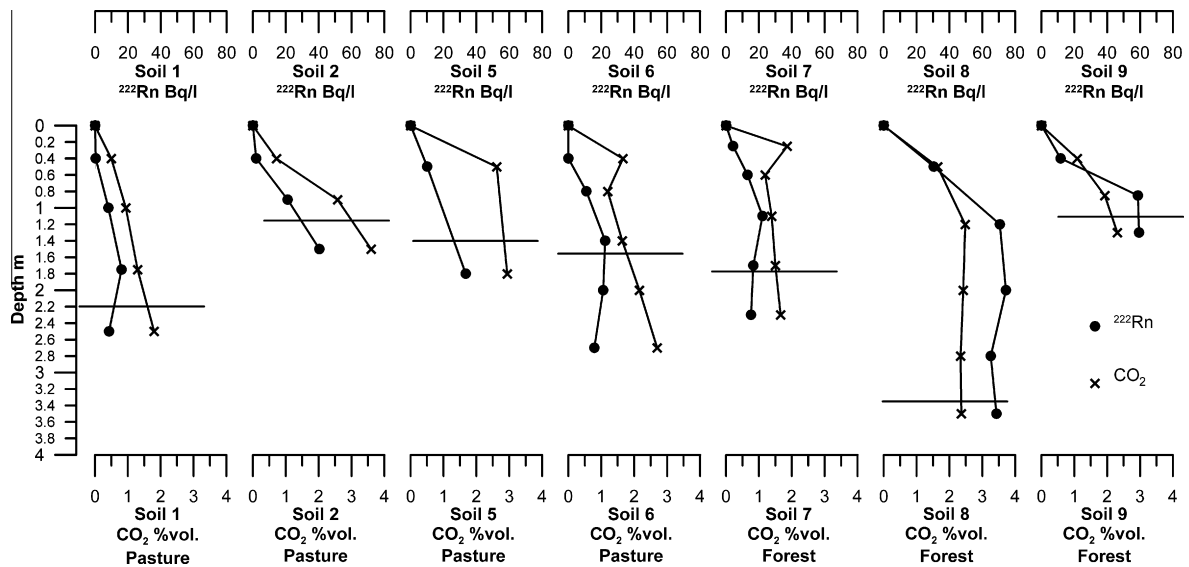


Fig. 3. Gas phase  $^{222}\text{Rn}$  activity and  $\text{CO}_2$  concentration for the soil boreholes. The horizontal lines represent the soil-epikarst limit.

Table 1

$\text{CO}_2$  concentrations in soil boreholes and deep epikarst borehole for different land use (7.2001–8.2002) and  $\text{CO}_2$  concentration in underground river at baseflow (10.2003–8.2004). Minimal, maximal, mean values and amplitude are represented in vol.%.

Boreholes Land use	Soil 1 Pasture	Soil 2 Pasture	Soil 5 Pasture	Soil 6 Pasture	Soil 7 Forest	Soil 8 Forest	Soil 9 Forest	Mean	Epikarst deep	Underground river at baseflow
Depth of borehole (m)	2.90	1.60	1.90	2.70	2.30	3.80	1.40		15.0	
Mean (annual)	1.73	3.49	2.81	2.36	1.48	2.18	2.88	2.42	2.66	2.17
Min (annual)	0.31	0.66	0.87	0.77	0.36	1.10	0.68	0.68	1.58	1.91
Max (annual)	2.83	5.10	4.50	3.32	2.73	2.80	4.50	3.68	3.60	2.31
Amplitude	2.52	4.44	3.63	2.56	2.37	1.70	3.82	3.01	2.02	0.4

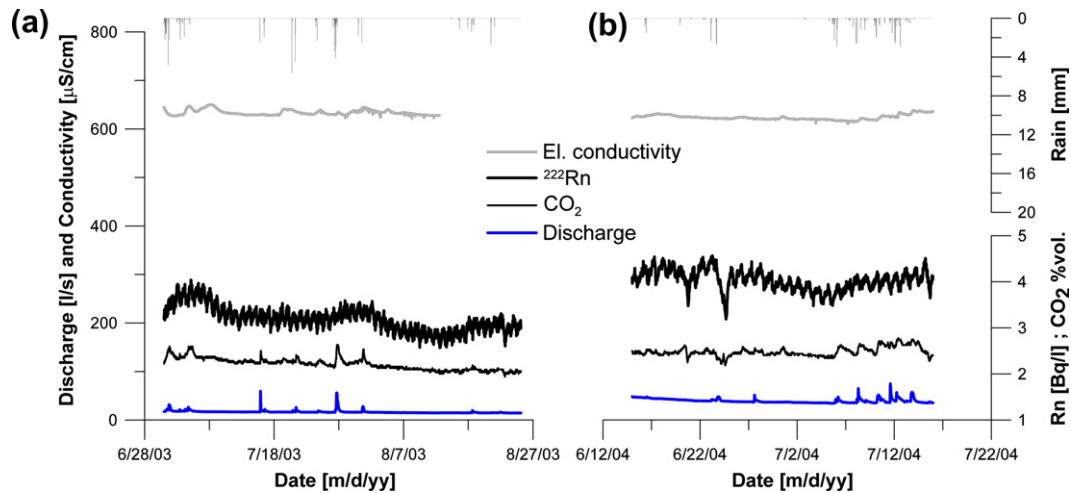


Fig. 4. Discharge, electrical conductivity,  $^{222}\text{Rn}$  activity and  $\text{CO}_2$  concentration during a baseflow period in summer 2003 (a) and summer 2004 (b) in the Milandre underground stream.

decreased again. The electrical conductivity decreased during the flood peaks.

The October 26th 2004 flood event corresponded to 84 mm rainfall during 2 days (Fig. 7b). The event can be separated in two successive flood events of increasing magnitude each linked to a rainfall event. The first small rainfall event led to a small  $\text{CO}_2$  increase of 0.7 vol.% (3.1 to vol.%) but no  $^{222}\text{Rn}$  increase was observed. During the second discharge peak, the  $^{222}\text{Rn}$  activity started to increase (from 3.3–10.1 Bq/l) 9 h after the beginning of the flood event and the maximum value (10.2 Bq/l) was reach

10 h after the discharge maximum. Similarly to the October 2002 event, the electrical conductivity decreased during the flood event.

## 6. Discussion

### 6.1. Origin and behaviour of $^{222}\text{Rn}$

Although only a limited number of soil gas measurements were made and the sampling locations were not distributed

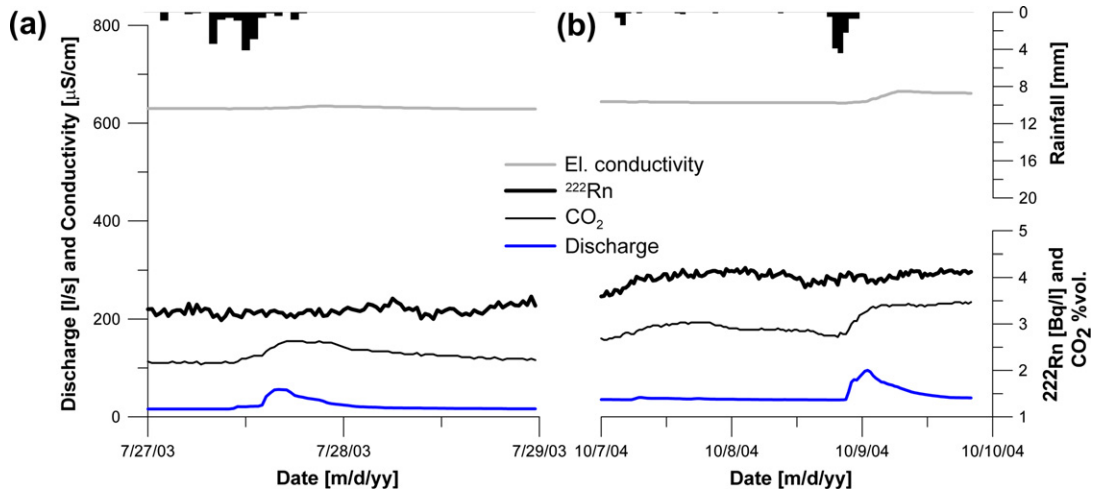


Fig. 5. Discharge, electrical conductivity, <sup>222</sup>Rn activity and CO<sub>2</sub> concentration during small flood event in July 2003 (a) and October 2004 (b) in the Milandre underground stream.

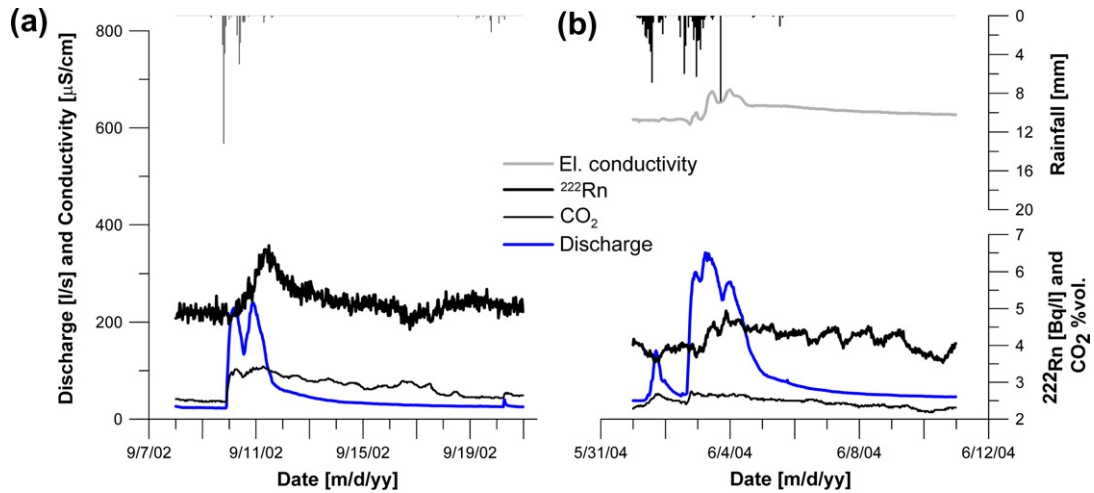


Fig. 6. Discharge, electrical conductivity, <sup>222</sup>Rn activity and CO<sub>2</sub> concentration during medium flood events in September 2002 (a) and July 2004 (b) in the Milandre underground stream.

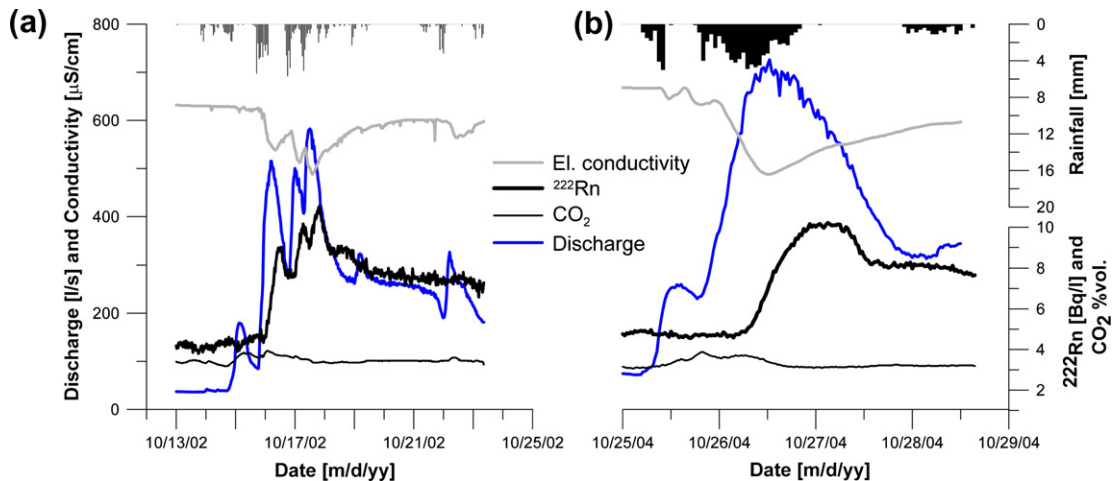


Fig. 7. Discharge, electrical conductivity, <sup>222</sup>Rn activity and CO<sub>2</sub> concentration during large flood events in October 2002 (a) and October 2004 (b) in the Milandre underground stream.

**Table 2**

Summary of the effect of flood events of different intensity on  $\text{CO}_2$ ,  $^{222}\text{Rn}$  and electrical conductivity in the Mildanrine underground stream. n.c. no significant change. n.m. not measured. Calculated contribution of freshly infiltrated event water ( $f_E$ ), water stored in the soil zone ( $f_S$ ) and water stored below the soil zone within limestone ( $f_L$ ) water in % and as an equivalent water column in mm distributed over the entire catchment area.

Event	Max. discharge L/s	$\Delta\text{CO}_2$ %	$\Delta^{222}\text{Rn}$ Bq/L	$\Delta\text{Cond}$ uS/cm	$f_E$ % (mm water column)	$f_S$ % (mm water column)	$f_L$ % (mm water column)	$f_{S;\text{max}}$ %
Small 1 (July)	55	+0.5	n.c.	n.c.				
Small 2 (October)	95	+0.7	n.c.	n.c.				
Medium 1 (September)	229	+0.9	+1.8	n.m.	0 (0)	6 (0.7)	94 (10.9)	22
Medium 2 (June)	341	+0.3	+1.0	+62	0 (0)	4 (0.8)	96 (17.9)	11
Large 1 (October)	Up to 579	+0.6	+6.8	-139	11 (5.1)	35-43 (16.3-20.1)	46-54 (21.4-25.1)	65
Large 2 (October)	730	+0.8	+5.5	-179	18 (4.7)	25-38 (6.8-10.1)	44-57 (11.9-15.2)	53

representatively over the entire catchment area, the comparison of soil gas and groundwater  $^{222}\text{Rn}$  activities can provide insight into the origin of  $^{222}\text{Rn}$  in the karst system. Using the average of the maximum  $^{222}\text{Rn}$  activity in each profile (37.4 Bq/L) and the Henry coefficient at 10 °C, an equilibrium aqueous phase  $^{222}\text{Rn}$  activity of 13.1 Bq/L is obtained. This value is substantially higher than  $^{222}\text{Rn}$  activity during baseflow (average of 3.8 Bq/L) when water is expected to predominantly originate from the fissured limestone volumes. This observation confirms that  $^{222}\text{Rn}$  is predominantly produced in the soil zone due to the enrichment of radionuclides in the soil during weathering. This conclusion is consistent with previous laboratory studies (Tadolini and Spizzico, 1998) and the high  $^{226}\text{Ra}$  activity in soils in the western Swiss Jura compared to the underlying limestone (Surbeck, 1992; Von Gunten et al., 1996). However, the sustained presence of  $^{222}\text{Rn}$  during base flow despite its short half-life indicates that some production of  $^{222}\text{Rn}$  occurs in the limestone. It is unlikely that  $^{222}\text{Rn}$  during base flow originates from the soil zone because a continuous decrease of the  $^{222}\text{Rn}$  activity during the base flow period would be expected, which is not observed. Furthermore, in the absence of precipitation little transfer of water from the soil zone to the cave is expected.

During flood events,  $^{222}\text{Rn}$  activities of up to 11.0 Bq/L were observed in the Mildanrine underground stream. The maximum  $^{222}\text{Rn}$  activities are close to the estimated soil water  $^{222}\text{Rn}$  activity, indicating that a significant portion of flood water had resided in the soil zone sufficiently long to acquire  $^{222}\text{Rn}$  activities close to

equilibrium. In contrast, during small flood events, no increase in the  $^{222}\text{Rn}$  activity was observed (Table 2) indicating that soil water does not participate in the small flood event. Based on the  $^{222}\text{Rn}$  activity, it can be estimated how long the water of small flood events had resided below the soil zone. The calculation assumes that water transiting through the soil zone acquires a  $^{222}\text{Rn}$  activity of 13.4 Bq/L as estimated above. It takes 25 days for the  $^{222}\text{Rn}$  activity to fall within the range of uncertainty ( $\pm 0.1$  Bq/L) of the background activity (3.8 Bq/L). This interval corresponds to the minimal period that the water has been stored below the soil zone until it arrives at the sampling point. During medium and large flood events, the  $^{222}\text{Rn}$  activity only increases with a delay with respect to the discharge increase while the  $\text{CO}_2$  concentration increases immediately. This finding confirms a soil origin of  $^{222}\text{Rn}$ . During the rising limb of the flood event, water having resided below the soil zone is flushed out before soil water rich in  $^{222}\text{Rn}$  arrives. Hence the  $^{222}\text{Rn}$  activities can provide valuable information on the time scale of water transfer from the land surface to the saturated part of karst system.

## 6.2. Origin and behaviour of $\text{CO}_2$

In contrast to the  $^{222}\text{Rn}$  activity, the  $\text{CO}_2$  concentration increased also during the small flood event (Table 2). During medium and large flood event both  $\text{CO}_2$  and  $^{222}\text{Rn}$  increased. However, the two parameters show a distinctly different temporal trend as becomes apparent when plotting the two parameters against discharge (Fig. 8).

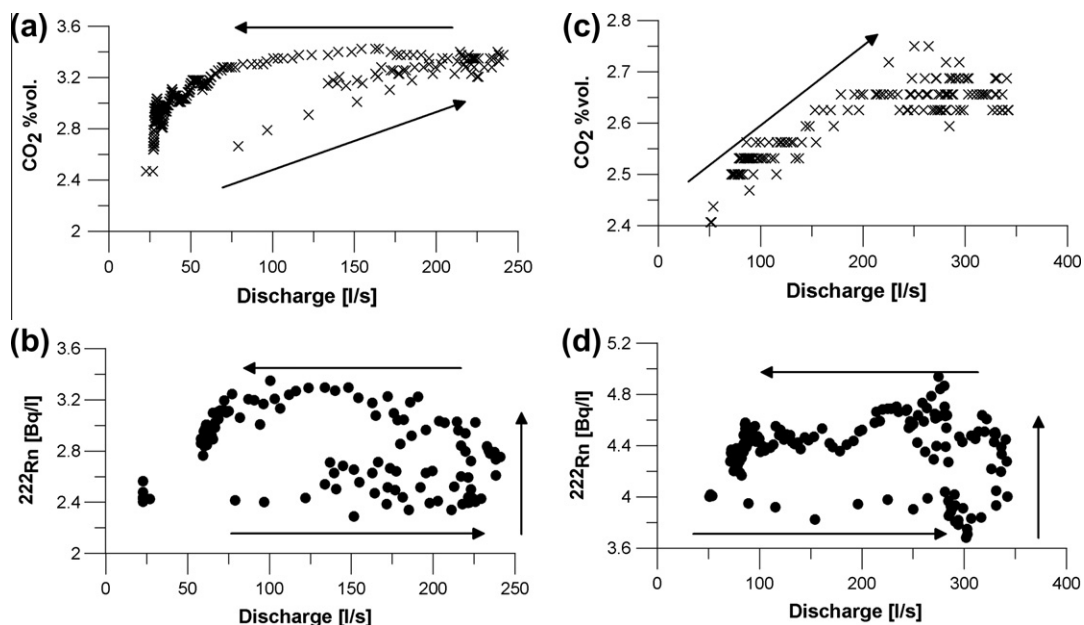


**Fig. 8.**  $\text{CO}_2$  (a) and  $^{222}\text{Rn}$  (b) behaviour as a function of discharge during a medium flood event in September 2002.  $\text{CO}_2$  (c) and  $^{222}\text{Rn}$  (d) behaviour as a function of discharge during a medium flood event in July 2004.

While the  $^{222}\text{Rn}$  activity only increased with a delay compared to the discharge, the  $\text{CO}_2$  concentration increased immediately. The increase of the  $\text{CO}_2$  concentration also during small flood event and the immediate increase during medium and large flood events indicate that the elevated  $\text{CO}_2$  concentration is associated with water stored below the soil zone. If the elevated  $\text{CO}_2$  concentration were due to the arrival of soil water, the two  $\text{CO}_2$  values would have to be more strongly associated with the  $^{222}\text{Rn}$  trend. A possible explanation for the  $\text{CO}_2$  trend is that baseflow water in the stream has lower  $\text{CO}_2$  levels due to gas loss compared to water stored in low permeability zones that will be mobilised during flood events. The  $\text{CO}_2$  trends are distinctly different from other studies where a decrease of the  $\text{CO}_2$  concentration occurred during flood events (Liu et al., 2004, 2007) or a  $\text{CO}_2$  increase was observed during the recession limb of the hydrograph rather than at the beginning of the flood peak as in our study (Vesper and White, 2004). The different  $\text{CO}_2$  behaviour at other sites may be due to the higher importance of concentrated infiltration at these sites compared to our site. For example, Vesper and White (2004) explained the delayed increase of  $\text{CO}_2$  by concentrated infiltration via sinkholes with limited interaction with soil followed by diffuse water from dispersed infiltration through  $\text{CO}_2$ -rich soil.

### 6.3. Quantitative data evaluation

Similarly as in other studies, the water arriving at the sampling point was partitioned into freshly infiltrated event water and pre-event water. During small and medium flood events, there was no evidence for a contribution of event water to discharge while during large flood events freshly infiltrated water amounted to 11–18% of the total discharge. These findings are compatible with a previous study at the same site (Perrin et al., 2003a), which obtained a freshly infiltrated water contribution of up to 10% for flood events of up to 400 L/min using a mixing model based on  $\delta^{18}\text{O}$  in water. In a study in Indiana, USA, a similar freshly infiltrated water contribution of 10.3% was observed (Lee and Krothe, 2001).

The pre-event water was further partitioned using the  $^{222}\text{Rn}$  data. Since  $^{222}\text{Rn}$  activities are at same time affected by decay and mixing in zones below the epikarst, it is not possible to independently calculate mixing ratios and residence times. In the calculation, it was assumed that the high  $^{222}\text{Rn}$  water from soil rapidly transits through the unsaturated zone and hence  $^{222}\text{Rn}$  decay is negligible. The calculated fraction of soil water has to be considered as a conservative estimate. Alternative calculations

assuming that all  $^{222}\text{Rn}$ -rich water has migrated below the epikarst zone at the end of the precipitation event lead to decay-corrected  $^{222}\text{Rn}$  activities above soil values for large flood events, which are not plausible. The calculations indicated that pre-event water during small and medium flood events predominantly consists of water stored below the soil zone either in the deeper epikarst or phreatic zone of aquifer (Table 2). A soil storage contribution of only 4–6% was obtained for medium flood events equivalent to a 0.7–0.8 mm water column over the whole catchment area (Table 2). In contrast, during large flood events, soil water contributed to 25–43% of the total discharge, corresponding to a water column of 6.8–20.1 mm. For individual samples, the maximum contribution of soil water was 53% and 65%, respectively for the two large flood events. A contribution of 6.8–20.1 mm of  $^{222}\text{Rn}$  rich water from soil to discharge is plausible given that the zone of high  $^{222}\text{Rn}$  production extends over a thickness of 1.1–3.4 m. The calculations demonstrate that soil-stored water can significantly contribute to discharge in karst system during high-flow events.

### 6.4. Conceptual model

Based on the observed  $^{222}\text{Rn}$  and  $\text{CO}_2$  trends and the calculated mixing ratios, a conceptual model of recharge and flow dynamics was developed for rain events of different intensity taking into account previous studies that highlighted the importance of water storage in the epikarst (Pronk et al., 2009; Williams, 2008). During base flow, the underground stream discharge corresponds essentially to slow drainage of low permeability phreatic zones with low  $^{222}\text{Rn}$  values and annual average  $\text{CO}_2$  concentrations. During small flood events (Fig 9a), only water that has been stored below the soil zones for a period larger than 25 days participates to discharge as indicated by stable  $^{222}\text{Rn}$  activities. Some  $^{222}\text{Rn}$ -rich soil water likely reaches the epikarst and increases the discharge from the epikarst to deeper zone by increasing the water level in epikarst zone. However, soil water does not break through all the way to the measurement point (Fig. 9a). During medium flow events (Fig. 9b), more  $^{222}\text{Rn}$ -rich soil water reaches the epikarst and some of it migrates through the unsaturated zone possibly along dissolution enlarged fissures after lateral movement in the epikarst. However, the dominant source of water is still water that had been stored below the soil zone. Finally, after strong rainfall, a large amount of soil water is flushed into the epikarst together with freshly infiltrated water. Preferential flow paths from the epikarst to the saturated zones are activated leading to a rapid

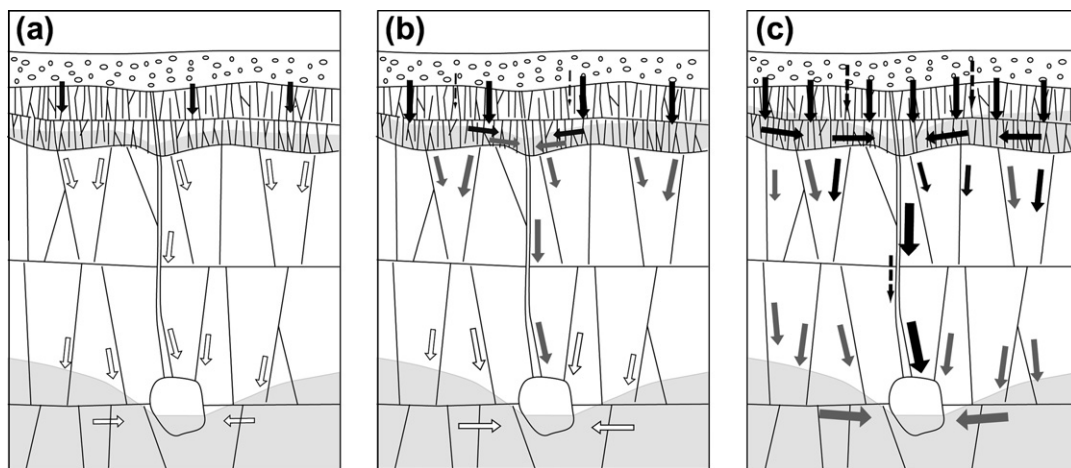


**Fig. 9.** Conceptual model of flow and  $^{222}\text{Rn}$  transport in karst aquifer during small (a), medium (b) and large (c) flood event. The figure illustrates the situation when maximum  $^{222}\text{Rn}$  activities are reached for a given event. White arrows: water with limestone  $^{222}\text{Rn}$  activity level, Black arrow: water with soil  $^{222}\text{Rn}$  activity level; grey arrows: water with intermediate  $^{222}\text{Rn}$  activity level; dashes arrow: event water.

transfer of this water to the saturated zone with little time for  $^{222}\text{Rn}$  decay (Fig. 9c). During such events, the highest  $^{222}\text{Rn}$  activities are observed.

## 7. Conclusion

The study demonstrates that  $^{222}\text{Rn}$  can provide detailed insight under which hydrological conditions, soil water or water having transited through the soil zone is rapidly transferred to the saturated zone.  $^{222}\text{Rn}$  is an ideal tracer for this purpose since it decays rapidly to limestone background levels when it is no longer in contact with the soil zone. While the study demonstrates the potential of  $^{222}\text{Rn}$  and  $\text{CO}_2$  as natural tracers, additional studies are necessary to characterise in more detail the input function of  $^{222}\text{Rn}$  and how it varies as function of precipitation intensity.

## Acknowledgements

This project was supported by the Swiss National Science Foundation and by the European Community 7th Framework Project GENESIS (226536). We thank the Jura Caving Club for access to the cave, M.E Wyniger and F. Bourret (Centre for Hydrogeology) for the lab and field work. We especially thank Dr. Jérôme Perrin for measurement of  $\text{CO}_2$  in soils and the comments of two reviewers that helped to improve the manuscript.

## References

- Bakalowicz, M., Blavoux, B., Mangin, A., 1974. Apports du traçage isotopique naturel à la connaissance du fonctionnement d'un système karstique – teneurs en oxygène 18 de trois systèmes des pyrénées. *France. J. Hydrol.* 23, 141–158.
- Baldini, J.U.L., Baldini, L.M., McDermott, F., Clipson, N., 2006. Carbon dioxide sources, sinks, and spatial variability in shallow temperate zone caves: evidence from Ballynamindra Cave, Ireland. *J. Cave. Karst Stud* 68 (1), 4–11.
- Batiot-Guilhe, C., Seidel, J.L., Jourde, H., Hebrard, O., Bailly-Comte, V., 2007. Seasonal variations of  $\text{CO}_2$  and  $\text{Rn-222}$  in a mediterranean sinkhole – spring (Causse d'Aumelas, SE France). *Int. J. Speleol.* 36 (1), 51–56.
- Bourges, F., Mangin, A., d'Hulst, D., 2001. Carbon dioxide in karst cavity atmosphere dynamics: the example of the Aven d'Orgnac (Ardeche). *CR. Acad. Sci.* 333 (11), 685–692.
- Caballero, E., Jimenez De Cisneros, C., Reyes, E., 1996. A stable isotope study of cave seepage waters. *Appl. Geochem.* 11 (4), 583–587.
- Chapman, J.B., 1992. Isotopic investigation of infiltration and unsaturated zone flow processes at Carlsbad cavern, New Mexico. *J. Hydrol.* 133, 343–363.
- Clever, H.L., 1979. Krypton, Xenon, Radon – Gas Solubilities IUPAC Solubility Data Series 2. Pergamon Press, Oxford, p. 357.
- Criss, R., Davison, L., Surbeck, H., Winston, W., 2007. Isotopic methods. In: Goldscheider, N., Drew, D. (Eds.), *Methods in Karst Hydrogeology*. Taylor & Francis, London, pp. 123–146.
- Eisenlohr, L., Surbeck, H., 1995. Radon as a natural tracer to study transport processes in a karst system. An exemple in the Swiss Jura. *CR. Acad. Sci.* 321 (2a), 761–767.
- Emblanch, C., Zuppi, G.M., Mudry, J., Blavoux, B., Batiot, C., 2003. Carbon 13C of TDIC to quantify the role of the unsaturated zone: the exemple of the Vauluse karst systems (Southeastern France). *J. Hydrol.* 279, 262–274.
- Falcone, R.A., Falgiani, A., Parisse, B., Petitta, M., Spizzico, M., Tallini, M., 2008. Chemical and isotopic ( $\delta\text{O-18}$  parts per thousand,  $\delta\text{H-2}$  parts per thousand,  $\delta\text{C-13}$  parts per thousand,  $\text{Rn-222}$ ) multi-tracing for groundwater conceptual model of carbonate aquifer (Gran Sasso INFN underground laboratory – central Italy). *J. Hydrol.* 357 (3–4), 368–388.
- Fernandez-Cortes, A., Sanchez-Moral, S., Cuezva, S., Canaveras, J.C., Abella, R., 2009. Annual and transient signatures of gas exchange and transport in the Castanar de Ibor cave (Spain). *Int. J. Speleol.* 38 (2), 153–162.
- Harmon, R.S., 1979. An isotopic study of groundwater seepage in the central kentucky karst. *Water Resour. Res.* 15 (2), 476–480.
- Hunkeler, D., Mudry, J., 2007. Hydrochemical methods. In: Goldscheider, N., Drew, D. (Eds.), *Methods in Karst Hydrogeology*. Taylor & Francis, London, pp. 93–122.
- Käss, W., 1998. Tracer technique in geohydrology. Balkema, Rotterdam, p. 589.
- Katz, B.G., Catches, J.S., Bullen, T.D., Michel, R.L., 1998. Changes in the isotopic and chemical composition of ground water resulting from a recharge pulse from a sinking stream. *J. Hydrol.* 211 (1–4), 178–207.
- Kovacs, A., Jeannin, P.Y., 2003. Hydrogeological overview of the Bure plateau, Ajoie, Switzerland. *Eclogae Geol. Helv.* 96 (3), 367–379.
- Lakey, B., Krothe, N.C., 1996. Stable isotopic variation of storm discharge from a perenial karst spring, Indiana. *Water Resour. Res.* 32 (3), 721–731.
- Lastennet, R., Mudry, J., 1987. Role of karstification and rainfall in the behavior of a heterogeneous karst system. *Environ. Geol.* 32 (2), 114–123.
- Laubenstein, M., Magaldi, D., 2008. Natural radioactivity of some red Mediterranean soils. *Catena* 76 (1), 22–26.
- Lee, E.S., Krothe, N.C., 2001. A four-component mixing model for water in karst terrain in south-central Indiana, USA. Using solute concentration and stable isotope as tracers. *Chem. Geol.* 179, 129–143.
- Liu, Z.H., Groves, C., Yuan, D.X., Meiman, J., 2004. South China karst aquifer storm-scale hydrochemistry. *Ground Water* 42 (4), 491–499.
- Liu, Z.H., Li, Q., Sun, H.L., Wang, J.L., 2007. Seasonal, diurnal and storm-scale hydrochemical variations of typical epikarst springs in subtropical karst areas of SW China: soil  $\text{CO}_2$  and dilution effects. *J. Hydrol.* 337 (1–2), 207–223.
- Mahler, B.J., Garner, B.D., 2009. Using nitrate to quantify quick flow in a karst aquifer. *Ground Water* 47 (3), 350–360.
- Maloszewski, P., Rauert, W., Trimborn, P., Herrmann, A., Rau, R., 1992. Isotope hydrological study of mean transit times in an alpine basin (Wimbachtal, Germany). *J. Hydrol.* 140, 343–360.
- Maloszewski, P., Stichler, W., Zuber, A., Rank, D., 2002. Identifying the flow systems in a karstic-fissured-porous aquifer, the Schnealpe, Austria, by modelling of environmental 18O and 3H isotopes. *J. Hydrol.* 256 (1–2), 48–59.
- Perrin, J., 2003. A conceptual model of flow and transport in a karst aquifer based on spatial and temporal variations of natural tracers. University of Neuchâtel, Neuchâtel, p. 187.
- Perrin, J., Jeannin, P.-Y., Zwahlen, F., 2003a. Epikarst storage in a karst aquifer: a conceptual model based on isotopic data, Milandre test site, Switzerland. *J. Hydrol.* 279 (1–4), 106–124.
- Perrin, J., Jeannin, P.-Y., Zwahlen, F., 2003b. Implications of the spatial variability of infiltration-water chemistry for the investigation of karst aquifer: a field study at the Milandre test site, Swiss Jura. *Hydrogeol. J.* 11, 673–686.
- Perrin, J., Jeannin, P.Y., Cornaton, F., 2007. The role of tributary mixing in chemical variations at a karst spring, Milandre, Switzerland. *J. Hydrol.* 332 (1–2), 158–173.
- Pronk, M., Goldscheider, N., Zopfi, J., Zwahlen, F., 2009. Percolation and particle transport in the unsaturated zone of a karst aquifer. *Ground Water* 47 (3), 361–369.
- Rank, D., Völk, G., Maloszewski, P., Stichler, W., 1992. Flow Dynamics in an Alpine Karst Massif Studied by Means of Environmental Isotopes. Isotope techniques in water resources development, International Atomy Agency, Vienna, pp. 327–343.
- Reardon, E.J., Allison, G.B., Fritz, P., 1979. Seasonal chemical and isotopic variations of soil  $\text{CO}_2$  at Trout Creek, Ontario. *J. Hydrol.* 43 (1–4), 355–371.
- Surbeck, H., 1992. Nature and extent of  $^{226}\text{Ra}$  anomaly in the western Swiss Jura. In: *International Symposium on Radon and Radon Reduction Technology*. EPA-600, Minneapolis, pp. 8–19.
- Surbeck, H., 1996. A radon-in-water monitor based on fast gas transfer membranes. In: *International Conference on Technologically Enhanced Natural Radioactivity (TENR) Caused by Non-uranium Mining*. Szczyrk, Poland, p. 10.
- Tadolini, T., Spizzico, M., 1998. Relation between “terra rossa” from the Apulia aquifer of Italy and the radon content of groundwater: experimental results and their applicability to radon occurrence in the aquifer. *Hydrogeol. J.* 6 (3), 450–454.
- Vervier, P., 1990. Hydrochemical characterization of the water dynamics of a karstic system. *J. Hydrol.* 121, 103–117.
- Vesper, D.J., White, W.B., 2004. Storm pulse chemographs of saturation index and carbon dioxide pressure: implications for shifting recharge sources during storm events in the karst aquifer at Fort Campbell, Kentucky/Tennessee, USA. *Hydrogeol. J.* 12, 135–143.
- Von Gunten, H.R., Surbeck, H., Rössler, E., 1996. Uranium series disequilibrium and high thorium and radium enrichments in karst formations. *Environ. Sci. Technol.* 30 (4), 1268–1274.
- Williams, P.W., 2008. The role of the epikarst in karst and cave hydrogeology: a review. *Int. J. Speleol.* 37 (1), 1–10.
- Yonge, C.J., 1985. Stable isotope studies of cave seepage water. *Chem. Geol.* 58, 97–105.